Journal of ELECTRICAL ENGINEERING, VOL. 57, NO. 1, 2006, 12–19

ANALYTICAL ANALYSIS OF ROTOR SLOT HARMONICS IN THE LINE CURRENT OF SQUIRREL CAGE INDUCTION MOTORS

Mohamed Yazid Kaikaa — Fatima Babaa
Abdelmalek Khezzar — Mohamed Boucherma *

This paper describes a new approach for analysing the effect of the space distribution of rotor bars in squirrel cage induction machines on the generation of rotor slot harmonics (RSH). An analytical expression of the stator current has been developed. The proposed expression is based on the linkage inductance expression derived using the winding function approach (WFA) and its decomposition into Fourier series. This approach describes the necessary relationship required for the presence of rotor slot harmonics and explains how the stator current is influenced by voltage unbalance. Simulations results have shown excellent match with theoretically predicted harmonic components.

K e y w o r d s: induction motor, rotor slot harmonics, voltage unbalance, Fourier series, diagnostics

1 INTRODUCTION

The squirrel cage induction motor has been used in all kinds of electric drives more often than other electric motors because of its reliability, robustness and simplicity of its construction. The classical theory of this electromechanical component is based on the assumption that the rotating mmf produced by stator winding excitation is sinusoidally distributed in space and that the rotor mmf due to the slip frequency induced currents is similarly distributed. This condition would only exist, however, if the surfaces of the stator and rotor were both smooth, and the windings were sinusoidally distributed on them. In the real machine the windings are placed in slots and therefore the resulting mmf and flux density distributions are not sinusoidal but contain, apart from the fundamental wave, a series of space harmonics.

The space harmonics effects must be considered precisely during the design process of the induction machine to achieve good motor performance. These effects are of many kinds: asynchronous crawling, locking and synchronous crawling, magnetic noise, vibration and speed ripples. On the other hand the space harmonics have also a great influence on the harmonic content of stator currents. Several authors [1-3] have shown that, as a result of the nature of the rotor cage winding, all space harmonics from the stator side will be reflected by the rotor and occur only at high frequencies in the stator current spectrum. These harmonics known as rotor slot harmonics (RSH) have found application in modern speed estimation techniques [4–6]; in addition, recent works have shown that it is possible to use them to monitor some mechanical and electrical faults.

Toliyat et al [7] have proposed the detection of air gap eccentricity in induction machines by measuring the harmonic content in the stator current spectrum. By means of the winding function approach all the space harmonics were taken into account. Vas [3] has presented a formula for computing the frequency components in the stator current which is due to air gap eccentricity. The frequency components are found to be function of the fundamental stator frequency, number of rotor slots, slip, type of eccentricity and stator mmf time harmonics.

Thomson *et al* [8,9] have investigated inter-turn stator faults by looking at RSH in the stator current spectrum. Their results showed that one of the RSH in stator current spectrum could be used to detect shorted turns in a stator coil. However, recent works [10, 11] have led to conclude that RSH can not be used as a specific sign on the occurrence of inter-turn short circuits in stator windings.

The effects arising due to broken rotor bars have been carefully studied in [12]. The results of this study showed that the two classical components $(1 \pm 2ks)f$ are not the only effect due two rotor broken bars. There are other frequencies induced in the stator current around all RSH which can give more information about rotor asymmetry.

In this paper, the authors propose a new approach to investigate the effect of space distribution of rotor bars in a squirrel cage induction machine on the generation of RSH. The main task is to present an analytical approach of stator current frequency components in order to analyse in a more efficient way the information given by the stator current for the detection of voltage unbalance. At

* Electrical Laboratory of Constantine "LEC", Department of Electrical Engineering, Mentouri University – Constantine, 25000 Constantine, Algeria, E-mail: akhezzar@yahoo.fr

ISSN 1335-3632

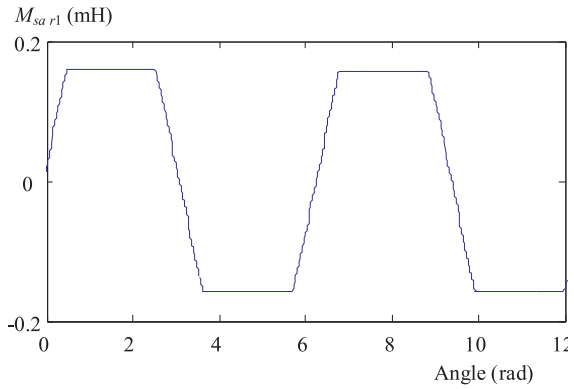

Fig. 1. Mutual inductance $M_{sa\,r1}$

the beginning, frequency components of the stator current for a healthy machine are analytically calculated. In the second step, the proposed study was extended to calculate the frequency components of the stator current under an unbalanced supply. The proposed approach is based on the Park mesh model and the linkage inductance matrix derived using the winding function approach (WFA) and developed into its Fourier series.

2 DETERMINATION OF THE MUTUAL INDUCTANCE MATRIX RESOLVED INTO ITS FOURIER SERIES

According to the winding function theory the mutual inductance between any two windings (i) and (j) in any electric machine can be computed by the following equation [13]:

$$L_{ij}(\varphi) = \mu_0 L\, r \int_0^{2\pi} \frac{n_i(\varphi,\theta) N_j(\varphi,\theta)}{e(\varphi,\theta)} \mathrm{d}\theta \qquad (1)$$

where: φ is the angular position of the rotor with respect to some stator reference, θ is a particular angular position along the stator inner surface, e is the air gap function, L is the length of stack and r is the average radius of the air gap. $n_i(\varphi,\theta)$ is the winding distribution of coil i; it is introduced to describe the considered coil, and $N_j(\varphi,\theta)$ is the winding function of coil j; it represents the mmf of the air- gap produced by a unit current flowing in the considered coil.

Consider an induction machine having three symmetrical stator phases and N_r rotor bars. Figure 1 shows the mutual inductance $M_{sa\,r1}$ between the first stator phase (a) and the first rotor loop. This implies that the mutual inductance matrix presents harmonics with respect to the electrical angle θ. Consequently, this matrix can be resolved into its Fourier series [12], [14]:

$$[M_{sr}] = \sum_{h=1}^{\infty} M_{sr\,h} \times$$

$$\begin{bmatrix} \cos(h(\theta+\varphi_h)) & \dots & \cos(h(\theta+\varphi_h+ka)) & \dots \\ \cos\big(h(\theta+\varphi_h) - \frac{2\xi_h\pi}{3}\big) & \dots & \cos\big(h(\theta+\varphi_h+ka) - \frac{2\xi_h\pi}{3}\big) & \dots \\ \cos\big(h(\theta+\varphi_h) + \frac{2\xi_h\pi}{3}\big) & \dots & \cos\big(h(\theta+\varphi_h+ka) + \frac{2\xi_h\pi}{3}\big) & \dots \end{bmatrix} \qquad (2)$$

where:
$a = p\frac{2\pi}{N_r}$ is the electrical angle of a rotor loop,
φ_h is the initial phase angle,
$h = 1$ and $h = (6\nu \pm 1)_{\nu=1,2,\dots}$,
$\xi_h = \begin{cases} +1 & \text{if } h \in F, \\ -1 & \text{if } h \in B \end{cases}$
$F = \{1, 7, 13, 19, \dots\}$ is the set of forward components,
$B = \{5, 11, 17, \dots\}$ is the set of backward components.

3 CURRENT FREQUENCY COMPONENTS FOR HEALTHY INDUCTION MACHINE WITH BALANCED SUPPLY

If a symmetrical three phase stator winding of a squirrel cage induction motor is supplied by a symmetrical voltage system, a forward rotating field is induced in its air gap.

The rotor currents which flow in the rotor loops as a result of the forward field can be expressed as:

$$[i_{r,k}] = \begin{bmatrix} \vdots \\ I_{rm}\cos(s\omega_s t - ka - \gamma) \\ \vdots \end{bmatrix} \qquad (3)$$

where: s is the slip, γ is the initial phase angle, I_{rm} is the maximum value of the current.

The stator flux equations in vector matrix form can be written as:

$$[\psi_{3s}] = [L_s] \cdot [i_{3s}] + [M_{sr}] \cdot [i_{rk}]\,. \qquad (4)$$

Park's transform is a well-known three-phase to two-phase transform in machine analysis. The transformation equation for the stator windings is of the form

$$[X_{sodq}] = \begin{bmatrix} X_{so} & X_{sd} & X_{sq} \end{bmatrix}^t = \big[P_3(\theta_s)\big]^t \big[X_{3s}\big] \qquad (5)$$

where the *odq* transformation matrix is defined as

$$\big[P_3(\theta_s)\big] = \sqrt{\frac{2}{3}} \begin{pmatrix} 1/\sqrt{2} & \cos(\theta_s) & -\sin(\theta_s) \\ 1/\sqrt{2} & \cos(\theta_s - 2\pi/3) & -\sin(\theta_s - 2\pi/3) \\ 1/\sqrt{2} & \cos(\theta_s + 2\pi/3) & -\sin(\theta_s + 2\pi/3) \end{pmatrix} \qquad (6)$$

here θ_s is the angular displacement between the Park reference and the first phase of the stator.

Transforming the above set of the stator flux to the Park reference frame using (5) we obtain

$$\big[\psi_{sodq}\big] = \big[L_{sc}\big] \cdot \big[i_{sodq}\big] + \big[M_{srp}\big] \cdot \big[i_{rk}\big] \qquad (7)$$

where

$$\left[L_{sc}\right]=\left[P_3(\theta_s)\right]^{-1}\cdot\left[L_s\right]\cdot\left[P_{3s}(\theta_s)\right]=\begin{bmatrix} L_{so} & 0 & 0\\ 0 & L_{sc} & 0\\ 0 & 0 & L_{sc}\end{bmatrix}. \quad (8)$$

Here, L_{so}, L_{sc} are the cyclic stator inductances.

$$\left[M_{srp}\right]=\left[P_3(\theta_s)\right]^{-1}\left[M_{sr}\right]=\sqrt{\frac{3}{2}}\sum_{h=1}^{\infty}M_{srh} \times\begin{bmatrix}\dots & 0 & \dots\\ \dots & \cos\left(\theta_s-h\xi_h(\theta+\varphi_h+ka)\right) & \dots\\ \dots & -\sin\left(\theta_s-h\xi_h(\theta+\varphi_h+ka)\right) & \dots\end{bmatrix}. \quad (9)$$

Substituting (8), (9) and (3) in (7), and eliminating the zero sequence, we obtain

$$\left[\psi_{sdq}\right]=\begin{bmatrix}L_s & 0\\ 0 & L_s\end{bmatrix}\cdot\begin{bmatrix}I_{sd}\\ I_{sq}\end{bmatrix} +\sqrt{\frac{3}{2}}\sum_{h=1}^{\infty}M_{srh}\begin{bmatrix}\dots & \cos\left(\theta_s-h\xi_h(\theta+\varphi_h+ka)\right) & \dots\\ \dots & -\sin\left(\theta_s-h\xi_h(\theta+\varphi_h+ka)\right) & \dots\end{bmatrix} \times\begin{bmatrix}\vdots\\ I_{rm}\cos(s\omega_s t-ka-\gamma)\\ \vdots\end{bmatrix}. \quad (10)$$

After performing simplifications, the stator flux equation became

$$\psi_{sd}=L_{sc}I_{sd}+\frac{1}{2}\sqrt{\frac{3}{2}}I_{rm}\left(\alpha\cos(\theta_s)+\beta\sin(\theta_s)\right) \quad (11)$$

$$\psi_{sq}=L_{sc}I_{sd}+\frac{1}{2}\sqrt{\frac{3}{2}}I_{rm}\left(\beta\cos(\theta_s)+\alpha\sin(\theta_s)\right) \quad (12)$$

where

$$\alpha=\sum_{h=1}^{\infty}\sum_{k=0}^{N_r-1}M_{srh}\Big\{\cos\left(s\omega_s t+h(\theta+\varphi_h)+k(h-1)\frac{2\pi p}{N_r}-\gamma\right) +\cos\left(s\omega_s t-h(\theta+\varphi_h)-k(h+1)\frac{2\pi p}{N_r}-\gamma\right)\Big\} \quad (13)$$

$$\beta=\sum_{h=1}^{\infty}\sum_{k=0}^{N_r-1}M_{srh}\Big\{\sin\left(s\omega_s t+h(\theta+\varphi_h)+k(h-1)\frac{2\pi p}{N_r}-\gamma\right) -\sin\left(s\omega_s t-h(\theta+\varphi_h)-k(h-+1)\frac{2\pi p}{N_r}-\gamma\right)\Big\} \quad (14)$$

Expressions (13), (14) show that α and β are equal to zero except when

$$h=\pm1,\ h=\left(\pm\frac{\lambda N}{p}-1\right)_{\lambda=1,2,\dots}\text{ or }h=\left(\pm\frac{\lambda N}{p}+1\right)_{\lambda=1,2,\dots}$$

where p is the number of pole pairs, λ is a positive integer.

Since h can be only a positive integer and related to the order of harmonics present in the mutual inductance linkage matrix as described by (2), it follows that α and β are different from zero only when h belongs to the following set:

$$G=\Big\{h=1\cup\Big(h=\Big(\frac{\lambda N_r}{p}\pm1\Big)_{\lambda=1,2,3,\dots}\cap h=(6\nu\pm1)_{\nu=1,2,3,\dots}\Big)\Big\} \quad (15)$$

Considering the stator reference frame ($\theta_s=0$) and substituting θ by $\left((1-s)\omega_s t\right)$ in (11) and (12) leads to

$$\psi_{sd}=L_{sc}I_{sd}+\sum_{h\in G}^{\infty}\frac{1}{2}\sqrt{\frac{3}{2}}N_r M_{srh}I_{rm}\cos(2\pi f_{sh}t\pm h\varphi_h-\gamma), \quad (16)$$

$$\psi_{sq}=L_{sq}I_{sq}-\sum_{h\in G}^{\infty}\frac{1}{2}\sqrt{\frac{3}{2}}N_r M_{srh}I_{rm}\sin(2\pi f_{sh}t\pm h\varphi_h-\gamma). \quad (17)$$

Expression (16) and (17) show clearly that in addition to the fundamental component, there exist also the so called rotor slot harmonics of orders h and frequencies $f_{sh}(p,N_r,\lambda)$ with

$$f_{sh}(p,N_r,\lambda)=f_s\Big[\frac{\lambda N_r}{p}(1-s)\pm1\Big]. \quad (18)$$

These harmonic components are the direct consequence of the space distribution of rotor bars.

It should be mentioned that
$f_{sh1}(p,N_r,\lambda)=f_s\left[\frac{\lambda N_r}{p}(1-s)+1\right]$ are the frequencies related to the orders $h=\left(\frac{\lambda N_r}{p}+1\right)_{\lambda=1,2,3,\dots}$.
$f_{sh2}(p,N_r,\lambda)=f_s\left[\frac{\lambda N_r}{p}(1-s)-1\right]$ are the frequencies related to the orders $h=\left(\frac{\lambda N_r}{p}-1\right)_{\lambda=1,2,3,\dots}$.

By means of equation (5), the stator voltage in Park reference frame and the line current equations can be written as

$$\left[V_{sdq}\right]=\left[R_s\right]\cdot\left[I_{sdq}\right]+\frac{\mathrm{d}}{\mathrm{d}t}\left[\psi_{sdq}\right], \quad (19)$$

$$I_{sa}=\sqrt{\frac{2}{3}}I_{sd}. \quad (20)$$

Equation (20) shows that to calculate the stator current we need only the direct Park stator current component (I_{sd}).

From (19) and (16) the differential equation giving the direct component of Park stator current is

$$R_s I_{sd}+L_s+\frac{\mathrm{d}I_{sd}}{\mathrm{d}t}=\sqrt{\frac{3}{2}}V_m\cos(\omega_s t)+\sum_{h\in G}^{\infty}\frac{1}{2}\sqrt{\frac{3}{2}}N_r \times M_{srh}I_{rm}2\pi f_{sh}\sin\left(2\pi f_{sh}(p,N_r,\lambda)t\pm h\varphi_h-\gamma\right). \quad (21)$$

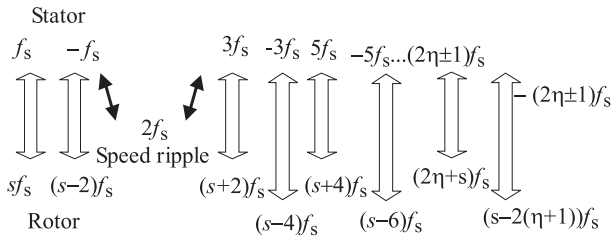

Fig. 2. Electromagnetic and mechanical phenomena in the stator and the rotor

The resolution of equation (21) leads to the analytical expression of the stator current

$$I_{sa} = \sqrt{\frac{2}{3}}\frac{V_m}{\sqrt{R_s^2+(L_s\omega_s)^2}}\cos(\omega_s t-\delta)+ \sum_{h\in G}^{\infty}\frac{\frac{1}{2}\sqrt{\frac{3}{2}}N_r M_{srh} I_{rm} 2\pi f_{sh}(p,N_r,\lambda)}{\sqrt{R_s^2+\big(L_s f_{sh}(p,N_r,\lambda)2\pi\big)^2}} \times \sin\big(2\pi f_{sh}(p,N_r,\lambda)t-\delta_h\pm h\varphi_h-\gamma\big) \quad (22)$$

with $\tan\delta = \frac{L_s\omega_s}{R_s}$ and $\tan\delta_h = \frac{L_s f_{sh}(p,N_r,\lambda)2\pi}{R_s}$.

4 CURRENT FREQUENCY COMPONENTS FOR A HEALTHY MACHINE WITH UNBALANCED VOLTAGE SUPPLY

As explained in [15], unbalance in a three phase voltage supply causes negative sequence currents (*ie* backward field) in the stator windings. The interaction of this negative sequence current with the fundamental frequency rotor currents produces a pulsating torque at double main frequency. This pulsating torque produces a speed ripple.

The rotor speed variation gives rise to other frequencies in the stator windings: $3f_s, 5f_s, \ldots, (2\eta+1)f_s$ (*ie* positive sequence currents) and $-3f_s, -5f_s, \ldots, -(2\eta+1)f_s \ldots$, (*ie* negative sequence currents) with $\eta = 1, 2.3.\ldots$. Consequently new harmonic components occur in the rotor side at: $(2+s)f_s, (s-4)f_s, (4+s)f_s, (s-6)f_s, \ldots$ and $(2\eta+s)f_s, (s-2(\eta+1)f_s$.

The electromagnetic and mechanical phenomena in the stator and the rotor can be summarized as shown in Fig. 2.

In this case, the rotor currents which flow in the rotor loops due to the negative and positive sequences currents are of the form

$$\big[I_{rk}\big] = \big[I_{rkp}\big] + \big[I_{rkn}\big] \quad (23)$$

where $\big[I_{rkp}\big] =$

$$= \begin{bmatrix} \vdots \\ I_{rmp}\cos\big((2\eta+s)\omega_s t - ka - \gamma_p\big) \\ \vdots \end{bmatrix}_{k=0,1,2,\ldots,N_r-1} \quad (24)$$

and $\big[I_{rkn}\big] =$

$$= \begin{bmatrix} \vdots \\ I_{rmn}\cos\big((2(\eta+1)-s)\omega_s t + ka - \gamma_n\big) \\ \vdots \end{bmatrix}_{k=0,1,2,\ldots,N_r-1} . \quad (25)$$

In the same manner as described above, the stator flux equation can be written as

$$\psi_{sd} = L_{sc}I_{sd} + \frac{1}{2}\sqrt{\frac{3}{2}}I_{rmp}\big(\alpha_p\cos(\theta_s)+\beta_p\sin(\theta_s)\big) + L_{sc}I_{sd} + \frac{1}{2}\sqrt{\frac{3}{2}}I_{rmn}\big(\alpha_n\cos(\theta_s)+\beta_n\sin(\theta_s)\big) \quad (26)$$

where

$$\alpha_p = \sum_{h=1}^{\infty}\sum_{k=0}^{N_r-1} M_{srh}\Big\{\cos\Big(\big((2\eta+s)\omega_s t + h(\theta+\varphi_h)\big) + k(h-1)\frac{2\pi p}{N_r} - \gamma_p\Big) + \cos\Big(\big((2\eta+s)\omega_s t - h(\theta+\varphi_h)\big) - k(h+1)\frac{2\pi p}{N_r} - \gamma_p\Big)\Big\} \quad (27)$$

$$\beta_p = \sum_{h=1}^{\infty}\sum_{k=0}^{N_r-1} M_{srh}\Big\{\sin\Big(\big((2\eta+s)\omega_s t + h(\theta+\varphi_h)\big) + k(h-1)\frac{2\pi p}{N_r} - \gamma_p\Big) - \sin\Big(\big((2\eta+s)\omega_s t - h(\theta+\varphi_h)\big) - k(h+1)\frac{2\pi p}{N_r} - \gamma_p\Big)\Big\} \quad (28)$$

$$\alpha_n = \sum_{h=1}^{\infty}\sum_{k=0}^{N_r-1} M_{srh}\Big\{\cos\Big(\big((2(\eta+1)-s)\omega_s t + h(\theta+\varphi_h)\big) + k(h+1)\frac{2\pi p}{N_r} - \gamma_n\Big) + \cos\Big(\big((2(\eta+1)-s)\omega_s t - h(\theta+\varphi_h)\big) - k(h-1)\frac{2\pi p}{N_r} - \gamma_n\Big)\Big\} \quad (29)$$

$$\beta_n = \sum_{h=1}^{\infty}\sum_{k=0}^{N_r-1} M_{srh}\Big\{\sin\Big(\big((2(\eta+1)-s)\omega_s t + h(\theta+\varphi_h)\big) + k(h+1)\frac{2\pi p}{N_r} - \gamma_n\Big) - \sin\Big(\big((2(\eta+1)-s)\omega_s t - h(\theta+\varphi_h)\big) - k(h-1)\frac{2\pi p}{N_r} - \gamma_n\Big)\Big\} \quad (30)$$

here also α_p, β_p, and β_n are different from zero only when h belongs to the following set:

$$G = \Big\{ h = 1 \cup \Big(h = \Big(\frac{\lambda N_r}{p} \pm 1 \Big)_{\nu=1,2,3,\ldots} \cap h = (6\nu \pm 1)_{\nu=1,2,3,\ldots} \Big) \Big\}. \quad (31)$$

Considering the stator reference frame ($\theta_s = 0$) and substituting θ by $\big((1-s)\omega_s t\big)$ in (26) leads to

$$\psi_{sd} = L_{sc} I_{sd} + \sum_{h\in G}^{\infty} \frac{1}{2}\sqrt{\frac{3}{2}} N_r M_{srh} I_{rmp} \cos\big(2\pi f_{shp}(p, N_r, \lambda, \eta)t \pm h\varphi_h - \gamma_p\big) + L_{sc} I_{sd} + \sum_{h\in G}^{\infty} \frac{1}{2}\sqrt{\frac{3}{2}} N_r M_{srh} I_{rmn} \cos\big(2\pi f_{shn}(p, N_r, \lambda, \eta)t \pm h\varphi_h - \gamma_n\big) \quad (32)$$

Expression (32) shows that in addition to the fundamental component, there exist also a series of high harmonics of frequencies $f_{shp}(p, N_r, \lambda, \eta)$ and $f_{shn}(p, N_r, \lambda, \eta)$.
Where

• the frequencies of the rotor slot harmonics which are caused by the positive sequence currents are

$$f_{shp1}(p, N_r, \lambda, \eta) = f_s\Big[\frac{\lambda N_r}{p}(1-s) + 1 + 2\eta\Big]$$

related to the orders $h = \Big(\frac{\lambda N_r}{p} + 1\Big)_{\lambda=1,2,3,\ldots}$, (33)

$$f_{shp2}(p, N_r, \lambda, \eta) = f_s\Big[\frac{\lambda N_r}{p}(1-s) - 1 - 2\eta\Big]$$

related to the orders $h = \Big(\frac{\lambda N_r}{p} - 1\Big)_{\lambda=1,2,3,\ldots}$, (34)

• the frequencies of the rotor slot harmonics which are caused by the negative sequence currents are

$$f_{shn1}(p, N_r, \lambda, \eta) = f_s\Big[\frac{\lambda N_r}{p}(1-s) + 1 + 2\eta\Big]$$

related to the orders $h = \Big(\frac{\lambda N_r}{p} - 1\Big)_{\lambda=1,2,3,\ldots}$, (35)

$$f_{shn2}(p, N_r, \lambda, \eta) = f_s\Big[\frac{\lambda N_r}{p}(1-s) - 1 - 2\eta\Big]$$

related to the orders $h = \Big(\frac{\lambda N_r}{p} + 1\Big)_{\lambda=1,2,3,\ldots}$. (36)

It is significant to note that the case of $\eta = 0$ corresponds to the case of neglected speed ripples. Finally, in the same manner as above, the stator current can be written as

$$I_{sa} = 2\sqrt{\frac{2}{3}} \frac{V_m}{\sqrt{R_s^2 + (L_s\omega_s)^2}} \cos(\omega_s t - \delta) + \sum_{h\in G}^{\infty} \frac{\frac{1}{2}\sqrt{\frac{3}{2}} N_r M_{srh} I_{rmp} 2\pi f_{shp}(p, N_r, \lambda, \eta)}{\sqrt{R_s^2 + (L_s f_{sh}(p, N_r, \lambda, \eta)2\pi)^2}} \times \sin\big(2\pi f_{shp}(p, N_r, \lambda, \eta)t - \delta_h \pm h\varphi_{hp} - \gamma\big) + \sum_{h\in G}^{\infty} \frac{\frac{1}{2}\sqrt{\frac{3}{2}} N_r M_{srh} I_{rmp} 2\pi f_{shn}}{\sqrt{R_s^2 + (L_s f_{sh}(p, N_r, \lambda, \eta)2\pi)^2}} \times \sin\big(2\pi f_{shn}(p, N_r, \lambda, \eta)t - \delta_h \pm h\varphi_{hn} - \gamma\big) \quad (37)$$

with $\tan\delta = \dfrac{L_s\omega_s}{R_s}$, $\tan\delta_{hp} = \dfrac{L_s f_{shp}(p.N_r, \lambda, \eta)2\pi}{R_s}$, $\tan\delta_{hn} = \dfrac{L_s f_{shn}(p.N_r, \lambda, \eta)2\pi}{R_s}$.

5 SIMULATIONS AND DISCUSSIONS

5.1 For balanced voltage

The simulated machine has 36 stator slots 28 bars, 2 poles and a rated power of 1.1 kW. The stator windings are connected in star. Simulation results were obtained using three phases, 380 V, 50 Hz ac source and were carried out at a slip around 0.038. The spectral estimates of stator currents have been normalized with respect to their respective fundamental components.

Figure (3) shows the spectral content of the stator current of the machine under healthy condition (balanced supply). In addition to the fundamental harmonic appear rotor slot harmonics.

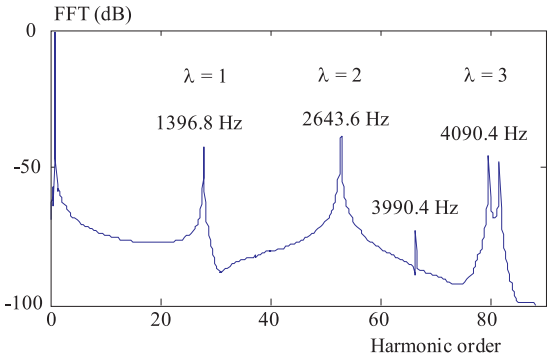

Fig. 3. Simulated, normalized FFT spectrum of machine stator current of induction machine having 28 rotor bars

Table 1. Stator current frequency components predicted by equations (15) and (18)

N_r	$\lambda = 0$	$\lambda = 1$	$\lambda = 2$	$\lambda = 3$
28	f_s	$f_{sh1}(1, 28, 1)$	$f_{sh2}(1, 28, 2)$	$f_{sh1}(1, 28, 3)$ & $f_{sh2}(1, 28, 3)$
29	f_s	X	$f_{sh1}(1, 29, 2)$	X
30	f_s	$f_{sh1}(1, 30, 1)$ & $f_{sh2}(1, 30, 1)$	$f_{sh1}(1, 30, 2)$ & $f_{sh2}(1, 30, 2)$	$f_{sh1}(1, 30, 3)$ & $f_{sh2}(1, 30, 3)$

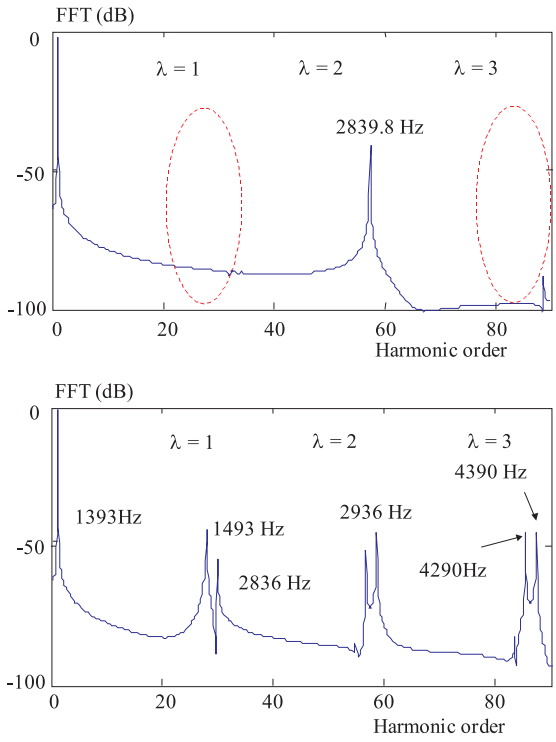

Fig. 4. Simulated, normalized FFT spectrum of machine stator current of induction machines top 29 bars, bottom 30 bars

Table 2. Stator current frequency components for machines with voltage unbalance and neglecting speed ripple effects

N_r	$\lambda = 0$	$\lambda = 1$	$\lambda = 2$	$\lambda = 3$
28	f_s	$f_{shp1}(1,28,1,0)$ & $f_{shn2}(1,28,1,0)$	$f_{shp1}(1,28,2,0)$ & $f_{shn2}(1,28,2,0)$	$f_{shp1}(1,28,3,0)$ & $f_{shn2}(1,28,3,0)$
29	f_s	X	$f_{shp1}(1,29,2,0)$ & $f_{shn2}(1,29,2,0)$	X
30	f_s	$f_{shp1}(1,30,1,0)$ & $f_{shn2}(1,30,1,0)$	$f_{shp1}(1,30,2,0)$ & $f_{shn2}(1,30,2,0)$	$f_{shp1}(1,30,3,0)$ & $f_{shn2}(1,30,3,0)$

In the case of ($\lambda = 1$) (*ie* the first two RSH), as predicted by (15) and (18) only one rotor slot harmonic can be seen on the stator current spectrum at $f_{sh1}(1,28,1) = 1396.8$ Hz and $h = \frac{28}{1} + 1 = 29$. The second rotor slot harmonic (at $f_{sh2}(1,28,1) = 1296.8$ Hz) did not show up because its order $h = \frac{28}{1} - 1 = 27$ does not belong to G, where G as described by equation (15) is $\{1, 29, 55, 83, 85, \dots\}$

In order to study the effects of rotor bar number on the generation of RSH, the 28 bar machine was replaced by two machines having 29,30 rotor bars respectively. The results are shown in Fig. 4 and are tabulated in Tab. 1.

Firstly, it can be observed that not all machines are capable of generating all RSH in the stator current. The simulated stator current spectrum of motors having 29 bars demonstrated this fact (Fig. 4).

On the other hand the simulated stator current spectrum of a motor having 30 bars shows that all RSH can be seen (Fig. 4).

5.2 For unbalanced voltage

In order to analyse with precision the effects arising due to voltage unbalance, the three machines were first simulated with 5 % of unbalanced supply and without speed ripple effects ($\eta = 0$), (*ie* with an infinite inertia value) [15]. The results are shown in Fig. 5 and are tabulated in Table 2.

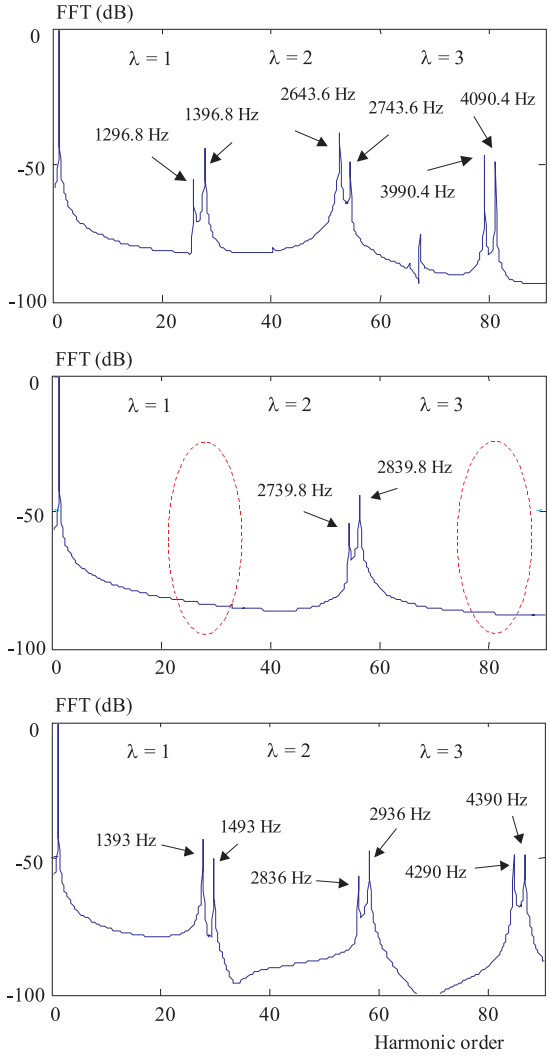

Fig. 5. Simulated, normalized FFT spectrum of machine stator current with 5 % supply unbalance and neglecting speed ripple effects from top 28, 29 and 30 bars

In the case of $N_r = 28$ bars and $\lambda = 1$, as predicted by (35) and (36) the order related to the $f_{shn1}(1,28,1,0) = 1396.8$ Hz component is $h = \frac{28}{1} - 1 = 27$, the order related to $f_{shn2}(1,28,1,0) = 1296.8$ Hz is $h = \frac{28}{1} + 1 = 29$.

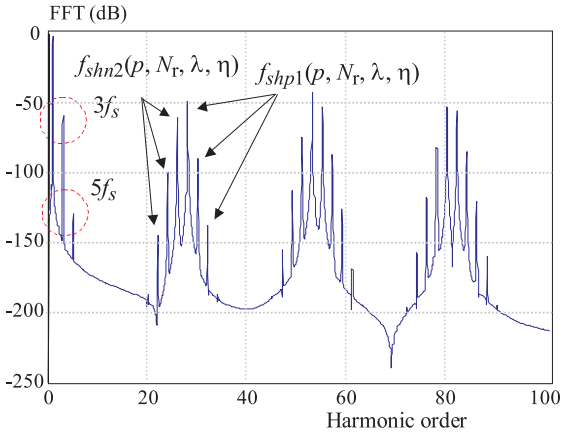

Fig. 6. Simulated, normalized FFT spectrum of machine stator current with speed ripple effects and 5 % supply unbalance (28 rotor bars)

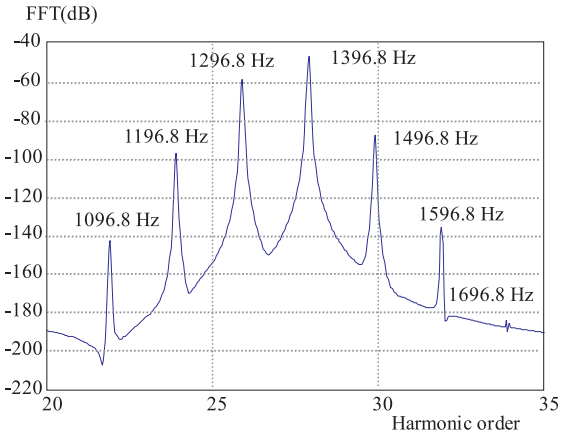

Fig. 7. Zoomed spectrum of machine stator current with speed ripple effects and 5 % supply unbalance (28 rotor bars)

Since only 29 belongs to G, only the $f_{shn2}(1, 28, 1, 0) = 1296.8$ Hz component can be induced by the negative sequence current (*ie* backward rotating field). Similarly, by means of equations (31), (33) and (34), we can prove that the creation of the $f_{shp1}(1, 28, 1, 0) = 1396.8$ Hz component in the stator current spectrum, as noted in Fig. 5, is due to the positive sequence current (*ie* forward rotating field).

By similar arguments, we can explain the creation of $f_{shn2}(1, 28, 2, 0) = 2739.8$ Hz and $f_{shp1}(1, 28, 2, 0) = 2839.8$ Hz components in the case of $N_r = 29$ bars and all RSH in the case of $N_r = 30$ bars respectively.

In addition, it is clear that the classical component at $3f_s$ is missing for all the above cases. So, it can be concluded that this component is related to speed ripple effects.

The machine having 28 bars was simulated next with speed ripple effects. The results are shown in Fig. 6. It is obvious that new frequency components are now present in the stator current spectrum at $f_{shp}(\lambda, p, N_r, \eta)$ and $f_{shn}(\lambda, p, N_r, \eta)$.

Figure 7 and Tables 3 and 4 summarize all the frequency components due to voltage unbalance for the cases of $(\lambda = 0)$ and $(\lambda = 1)$.

It is important to note that in the case of $\lambda = 1$, the harmonic components of frequencies

$$f_{shp2}(p, N_r, \lambda, \eta) = f_s \left[\frac{N_r}{p}(1 - s) - 1 - 2\eta\right] \text{ and}$$

$$f_{shn1}(p, N_r, \lambda, \eta) = f_s \left[\frac{N_r}{p}(1 - s) + 1 + 2\eta\right]$$

do not appear because their orders do not belong to G (Table 4).

6 CONCLUSIONS

In this paper the generation mechanism of rotor slot harmonics in stator current of a three phase squirrel induction machine was analysed. It has been shown that not all three phase induction motors are capable of generating all rotor slot harmonics. The presence of these harmonic components in the stator current spectra depends on the number of rotor bars, number of poles of the induction machine, and slip.

In addition, it has been demonstrated that the voltage unbalance is a potential source of generation of rotor slot harmonics in the stator currant. A new formulation was proposed in order to generalize and shed light on the necessary relationships required for the presence of these harmonic components.

Table 3. Stator current frequency components for healthy machine with voltage unbalance for $(\lambda = 0)$

η	$f_{shp}(p, N_r, \lambda, \eta)$	$f_{shn}(p, N_r, \lambda, \eta)$
0	$f_s = 50$ Hz	$-f_s$
1	$3f_s = 150$ Hz	$-3f_s$
2	$5f_s = 250$ Hz	$-5f_s$
3	$7f_s = 350$ Hz	$-7f_s$

Table 4. Stator current frequency components for healthy machine with voltage unbalance for $(\lambda = 1)$

η	$f_{shp1}(p, N_r, \lambda, \eta)$	$f_{shn2}(p, N_r, \lambda, \eta)$
0	$f_{shp1}(1, 28, 1, 0) = 1396.8$ Hz	$f_{shn2}(1, 28, 1, 0) = 1296.8$ Hz
1	$f_{shp1}(1, 28, 1, 1) = 1496.8$ Hz	$f_{shn2}(1, 28, 1, 1) = 1196.8$ Hz
2	$f_{shp1}(1, 28, 1, 2) = 1596.8$ Hz	$f_{shn2}(1, 28, 1, 2) = 1096.8$ Hz
3	$f_{shp1}(1, 28, 1, 3) = 1696.8$ Hz	$f_{shn2}(1, 28, 1, 3) = 996.8$ Hz

REFERENCES

[1] ALGER, P. L.: The Nature of Induction Machines, Gordon and Breach, London, UK, 1965.

[2] VAS, P.: Parameter Estimation, Condition Monitoring, and Diagnosis of Electrical Machines, Clarendon Press, Oxford, 1993.

[3] JOCSIMOVIC, G.—KJUROVIC, M.—PENMAN, J.: Cage Rotor MMF: Winding Function Approach, Power Engineering Review, IEEE **21** No. 4 (2001), 64–66.

[4] FERRAH, A.—BRADLEY, K. J.—ASHER, G. M.: An FFT-Based Novel Approach to Non-Invasive Speed Measurement in Induction Motors Drives, IEEE Transactions on Instrumentation and Measurement Technology **.41** No. 6 (1992), 797–802.

[5] ALLER, J. M.—RESTREPO, J. A.—BUENO, A.—GIMENEZ, M. I.—PESSE, G.: Squirrel Cage Induction Machine Model for the Analysis of Sensorless Speed Measurement Methods, Devices, Circuits and Systems, 1998, Proceedings of the Second IEEE International Caracas Conference on, 2-4 March 1998.

[6] NANDI, S.—AHMED, S.—TOLIYAT, H. A.—BHARADWAJ, R. M.: Selection Criteria of Induction Machines for Speed-Sensorless Drive Applications, IEEE Transactions on Industry Applications **39** No. 3 (2003), 704–712.

[7] TOLIYAT, H. A.—AREFEEN, M. S.—PARLOS, A. G.: A Method for Dynamic Simulation and Detection of Air Gap Eccentricity in Induction Machines, IEEE Trans. on Industry Application **32** No. 4 (1996), 910–918.

[8] THOMSON, W. T.: A Review of Online Condition Monitoring Techniques for Squirrel Cage Induction Motors — Past, Present and Future, Proceedings of the 1999 IEEE International Symposium on Diagnostic for Electrical Machines, Power Electronics and Drives, SDEMPED'99, 1999, pp. 3–18.

[9] THOMSON, W. T.—MCRAE, C. J.: On Line Current Monitoring to Detect Inter-Turn Stator Winding Faults in Induction Motors, Proceedings of the 24th Universities Power Engineering Conference, 1989, pp. 477–481.

[10] JOCSIMOVIC, G. M.—PENMAN, J.: The Detection of Inter-Turn Short-Circuits in the Stator Windings of Operating Motors, IEEE Transactions on Industrial Electronics **47** No. 5 (2000), 1078–1084.

[11] LU, Q. F.—RITCHIE, E.—CAO, Z. T.: Experimental Study of MCSA to Detect Stator Winding Inter-Turn Short Circuit Faults on Cage Induction Motors, In proc. International Conference on Electrical Machine ICEM'2004, Lódź, Poland, 5–8 Sep. 2004. CD proceeding.

[12] KHEZZAR, A.—KAIKAA, M. Y.—BOUCHERMA, M.: Analytical Investigation of Rotor Slot Harmonics in a Three Phase Induction Motor with Broken Rotor Bars, EPE 2005, Dresden, 11-14 Septemper, number 0350.pdf, CD proceeding.

[13] LUO, X.—LIAO, Y.—TOLIYAT, H. A.—EL-ANTABLY, A.—LIPO, T. A.: IEEE Transactions on Industry Applications.

[14] CHENY, C.—KAUFFMANN, J. M.: Information Losses in Decoupling Space Harmonics Effects for an Induction Drive, Mathematics and Computers in Simulation **46** (1998), 361–372.

[15] FILIPETTI, F.—FRANCESCHINI, G.—TASSONI, C.—VAS, P.: AI Techniques in Induction Machines Diagnosis Including the Speed Ripple Effect, Industry Applications, IEEE Transactions on **34** No. 1 (1998), 98–108.

Received 14 April 2005

Mohamed Yazid Kaikaa was born in Oran, Algeria, in 1977. He received the BSc degree in electrical engineering from the University of Constantine, Algeria, in 2002, and the MSc degree in electrical and computer engineering from the Electrical Engineering Institute of Constantine University, Algeria, in 2005. He is a member of the Research Laboratory of Electric Machines and Drives Control and Diagnosis of Constantine, Algeria. He currently works on his PhD thesis.

Fatima Babaa was born in Chambéry, France, in 1975. He received the BSc degree in electrical engineering from the University of Constantine, Algeria, in 2003, and the MSc degree in electrical and computer engineering from the Electrical Engineering Institute of Constantine University, Algeria, in 2005. He is a member of the Research Laboratory of Electric Machines and Drives Control and Diagnosis of Constantine, Algeria. He currently works on his PhD thesis.

Abdelmalek Khezzar (Ing, PhD), born in 1969, received the BSc degree in electrical engineering in 1993 from Batna University, Algeria, and PhD degree from INPL "Institut National Polytechnique de Lorraine" Nancy, France in 1997. He is currently an assistant professor at Mentouri University, Constantine, Algeria, in the Department of Electrical Engineering. His main research interests are power electronics and drives and analysis of electrical machines with special emphasis on fault diagnosis.

Mohamed Boucherma was born in Jijel, Algeria, in 1959. He received the BSc degree in Electrical Engineering, from the University of Annaba, Algeria, in 1985, the MSc degree in power system Engineering from the University of Strathclyde Scotland, in 1989, and the PhD in Electrical Engineering, from Sheffield University, England, in 1994. He is currently a lecturer at Mentouri University Constantine, Algeria, in the Department of Electrical Engineering. His main research interests are power systems and electrical machines.